2022 19th International Conference on Electrical Engineering, Computing Science and Automatic Control (CCE)
Mexico City, Mexico November 9-11, 2022

Adaptive Incremental Conductance as a Highly Efficient Maximum Power Point Tracking Algorithm for Photovoltaic Systems under Partial Shading

Jose L. Diaz-Bernabe
Chemistry Department
CINVESTAV IPN
CDMX, Mexico
ORCID: 0000-0002-0077-4693

Arturo Morales-Acevedo
Electrical Engineering Department
CINVESTAV IPN
CDMX, Mexico
ORCID: 0000-0003-0460-0823

***Abstract*—The Maximum Power Tracking (MPPT) Incremental Conductance (IC) and Adaptive Incremental Conductance (AIC) algorithms are simulated and compared for different shading patterns on a typical Photovoltaic (PV) System. The results show that the conventional IC algorithm misses the Global Maximum Power Point (GMPP) and achieves a low dynamic MPPT efficiency around 83% for PV strings under different critical shading conditions. However, the AIC algorithm, with optimized parameters, successfully tracks the GMPP and its dynamic MPPT efficiency is above 99.3% under similar shading conditions. Then, it is concluded that the AIC is far superior to the conventional IC algorithm, and it has a good performance like other soft computing and bio-inspired methods, but it is simpler to implement than those algorithms.**

***Index Terms*—Maximum power tracking, Incremental conductance, PV systems simulation**

I. Introduction

The Partial Shading Condition (PSC) is the situation whenever a group of PV modules of an array is receiving a reduced irradiance level while the remainder modules are well-lighted under a Uniform Irradiance Condition (UIC). Important shading sources are the traveling clouds, flying entities such as drones, bird flocks, planes, and other surrounding objects that darken a certain number of PV modules in an array. A shading condition reduces the magnitude of the PV system maximum power point because a shaded module quickly turns from a power generator into a power load. The shaded module supports a reverse voltage that increases beyond the breakdown voltage and the hot-spot effect might lead to a permanent damage. A widespread solution for PV arrays under shading conditions is the connection of a bypass diode in parallel to each PV module and a blocking diode in series to every PV string. The bypass diode restricts the reverse voltage to its forward polarization voltage and preserves the performance of the whole PV string under PSC, but the global cost increases as the PV system grows. In addition, the bypass diode adds a staircase shape to the *I-V* curve and a multi-peak sight to the *P-V* curve, as shown by the (normalized) curves in Fig. 1a and Fig. 1b.

Corresponding Author: amorales@solar.cinvestav.mx

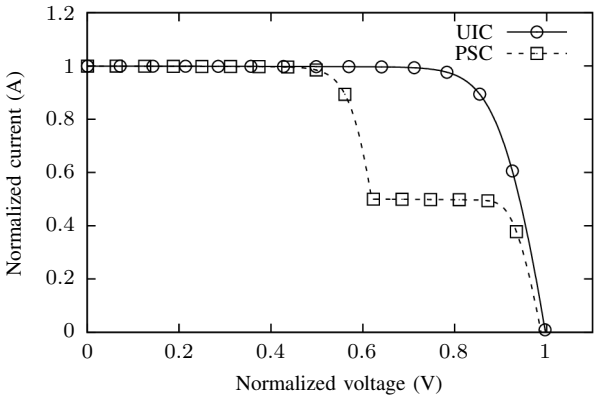

(a) Normalized *I-V* curves

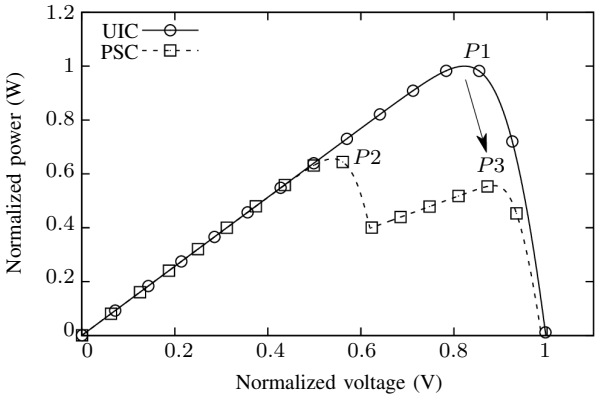

(b) Normalized *P-V* curves

Fig. 1: Characteristic curves under UIC and PSC.

Conventional Maximum Power Point Tracking (MPPT) algorithms, such as Perturb and Observe (P&O), proposed for a single power peak under UIC, might not track the Global Maximum Power Point (GMPP) well under PSC because it

would try to keep the uniform solar irradiance condition and consequently it would jump, for example, from *P1* to *P3* in Fig. 1b, but *P3* does not correspond to the GMPP under this specific partial shading condition.

Fig. 2 shows the schematics of a PV system with a single MPPT structure that directly modifies the duty-cycle d_k of the power converter to achieve the MPPT. It represents the first part of a two-stage grid connected inverter which links the PV string with the MPPT controller. In previous reports, [1]–[5] several improved conventional algorithms and new methods have been proposed for tracking the maximum power point in PV systems under PSC. Different methods of soft computing such as fuzzy logic, bio-inspired algorithms, and neural networks among others, have been proposed for tracking the GMPP in PV systems under PSC as an optimization problem solution [6]–[8]. However, the maximum power tracking efficiency advantage for these methods is not clearly verified or compared to other improved methods. Hybrid algorithms make a soft method work together with a conventional MPPT algorithm in trying to obtain the GMPP, and so the number of required parameters increases, and the implementation becomes more complex. Two-stage algorithms involve a voltage sweep strategy to guess the nearby voltages where a GMPP might appear, and at this latest point a conventional MPPT algorithm looks for the GMPP and determines it.

In this work, the behavior of a PV system under different critical shading profiles is simulated and analyzed. The theoretical GMPP's are tracked by means of the conventional IC and the improved AIC algorithms [9], and their MPPT efficiencies are compared. The main purpose is to confirm that conventional algorithms such as the IC (or P&O) have a very poor performance under shading conditions, but the improved adaptive algorithms, such as the AIC, are far superior and have similar tracking efficiencies (above 95%) as bio-inspired and neural-network algorithms under shading conditions.

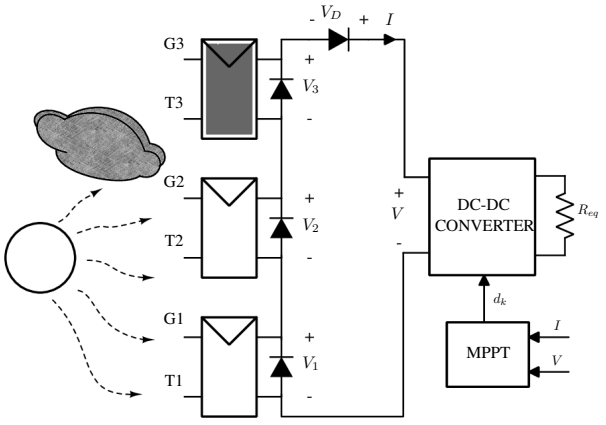

Fig. 2: PV system with a single-loop MPPT structure under PSC.

II. PV STRING UNDER SHADING CONDITIONS

The equivalent circuit for a PV module with a bypass diode is shown in Fig. 3. The circuit involves: a dependent current

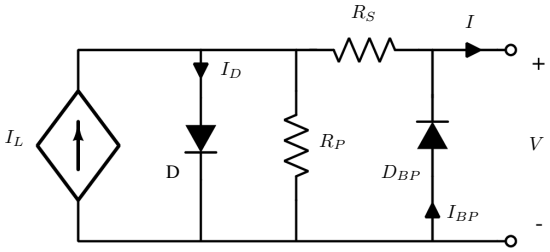

Fig. 3: Equivalent circuit of a PV module with a bypass diode.

source I_L, a diode D which models the diffusion and carrier recombination in dark conditions, a series resistance R_S and a parallel resistance R_P which represent the power losses inside the PV module. Notice the bypass diode $\mathrm{D_{BP}}$ included in this circuit.

The module output current I as a function of the voltage V is approximated by:

$$I = I_L - I_S \exp\left(\frac{V + IR_S}{AN_S V_{Th}}\right) - \frac{V + IR_S}{R_P} + I_{BP} \qquad (1)$$

where I_S represents the cell diode saturation current, A is the diode quality factor, N_S is the number of cells in series, V_{Th} is the thermal voltage at temperature T, and I_{BP} is the bypass diode current.

The photo-current I_L depends upon the cell area, solar irradiation level, and cell temperature. Once the cell area has been determined by design and manufacturing processes, the photocurrent is strongly affected by solar irradiance G (W/m^2) and cell temperature T_{cell}. I_L is proportional to the cell photocurrent (I_{L0}) measured under Standard Test Conditions[1] (STC):

$$I_L = I_{L0}\left(\frac{G}{1000}\right)\left[1 + K_{isc}\left(T_{cell} - T_{ref}\right)\right] \qquad (2)$$

As shown in [10], [11] the diode dark current I_0 is intensely affected by the cell temperature at a given solar irradiance:

$$I_S = I_0\left(\frac{T_{cell}}{T_{ref}}\right)^{\frac{3}{A}} \exp\left(-\frac{qE_g}{Ak}\left[\frac{1}{T_{cell}+273} - \frac{1}{T_{ref}+273}\right]\right) \qquad (3)$$

where I_0 is the diode dark current in STC, $k = 1.3806504 \times 10^{-23}$ J/K is the Boltzmann constant, and $q = 1.602176 \times 10^{-19}$ C is the electron charge. The current equation for the bypass diode is approximated by:

$$I_{BP} \approx I_{S:BP} \exp\left(-\frac{V}{A_{BP} V_{Th}}\right) \qquad (4)$$

where $I_{S:BP}$ is the saturation current and A_{BP} is the bypass diode quality factor.

As shown in [12], a generalized model for a PV array with *M-N* serial-parallel modules is developed by applying the electrical circuit serial-parallel rules to the current sources and resistors in the circuit of Fig. 3. However, even though this technique provides a comprehensive behavior of a PV array

[1]STC: G=1000 W/m^2, $T_{ref} = 25$C, AM=1.5

(or PV string), it is not suitable to understand its behavior under several shading scenarios. Then, the equation system in (5) is used to describe the PV string shown in Fig. 2.

$$\begin{aligned} V_1 + V_2 + V_3 + V_D - V &= 0 \\ I_1(V_1) - I_2(V_2) &= 0 \\ I_1(V_1) - I_3(V_3) &= 0 \\ I_1(V_1) - I_D(V_D) &= 0 \\ I_1(V_1) - I(V) &= 0 \end{aligned} \tag{5}$$

where each I_n is estimated by means of Eq. (1).

III. Incremental Conductance MPPT algorithms

Let us remember that the direct Incremental Conductance (IC) algorithm adjusts the duty-cycle d_k of the power converter every $k-th$ sampling cycle according to:

$$\begin{aligned} d_k &= d_{k-1} - d_{step}\text{sign}\left(\frac{I_k}{V_k} + \frac{\Delta I}{\Delta V}\right) \\ d_k &= [0,1] \end{aligned} \tag{6}$$

where d_{step} is a predetermined duty-cycle correction term, and the sign function determines if that quantity must be added or subtracted from previous duty-cycle. According to the switching converter theory [13], the duty-cycle d_k might belong to the closed interval between zero and one.

The direct Adaptive Incremental Conductance (AIC) algorithm [14] adjusts the duty-cycle d_k of the power converter every $k-th$ sampling cycle according to:

$$\begin{aligned} d_k &= d_{k-1} - N_{AIC}G_v \\ G_v &= \frac{I_k}{V_k} + \frac{\Delta I}{\Delta V} \\ d_k &= [0,1] \end{aligned} \tag{7}$$

where G_v is the Generalized Conductance function having units of Ω^{-1}, and N_{AIC} in units of Ω is a parameter tuned during the design stage and it determines the maximum value of the correction term.

As described in [15] the MPPT efficiency η_{mppt} allows us to evaluate the power tracking efficiency according to:

$$\eta_{mppt} = \frac{\int_0^T P(t)\,dt}{\int_0^T P_{max}(t)\,dt} \times 100 \quad [\%] \tag{8}$$

where $P(t)$ is the actual power of the PV system array when a given MPPT algorithm is used, $P_{max}(t)$ is the ideal maximum power of the PV array and T is the time interval for which the evaluation takes place.

IV. Simulation Results

Table I shows the main parameters of a typical commercially available PV module used to assemble large PV systems. In addition, Table II shows the essential parameters in STC of some grid-connected PV strings configurations.

A simulation model for the three module PV system (first row in Table II) shown in Fig. 2 was developed in Ngspice by using a behavioral modeling approach [17], [18]. The PV module with a bypass diode shown in Fig. 3 was implemented with the parameters given in Table I.

TABLE I
Specifications of a typical 245W PV Module [16]

Parameter	Symbol	Value
Voltage at MPP (V)	V_M	30.5
Current at MPP (A)	I_M	8.04
Open-Circuit Voltage (V)	V_{oc}	37.3
Short-circuit current (A)	I_{SC}	8.52
Series Cell number	N_S	60

TABLE II
Parameters for grid-connected PV string configurations

PV modules	Voltage at MPP *(V)*	Current at MPP *(A)*	Power *(W)*
3	91.5	8.04	735
5	150	8.04	1226
10	300	8.04	2452
12	360	8.04	2940

Fig. 4 shows the curves of a PV string receiving the irradiance levels *G1=G2=G3=1* Sun[2] under UIC. The current against voltage behavior is similar to that of a single PV module, but the open-circuit voltage is multiplied by three in Fig. 4a. Like a single PV module under UIC, there is a single GMPP at *P1* so the MPPT algorithm might find it with relatively little effort, see Fig. 4b. As shown in Fig. 4c and Fig. 4d, each PV module voltage varies from zero to its open-circuit voltage and the PV string voltage is equally distributed among the number of PV modules.

Fig. 5 shows the characteristics of a PV system under a shading condition where two PV modules receive the irradiance levels *G1=G2=1.0* Sun and one PV module receives an irradiance level *G3=0.5* Sun. Because the shading condition involves two irradiance levels, the *I-V* curve seen in Fig. 5a contains two current levels and the *P-V* curve in Fig. 5b shows two power peaks. The GMPP is at the left-side of the *P-V* curve, so that a MPPT algorithm might struggle to find *P2* or even it would not find it. The magnitude of *P2* in Fig. 5b is less than that of *P1* in Fig. 4b, meaning that the shading condition causes a reduction of the generated maximum power. Because the shaded PV module has a negative value generated by the bypass diode, the PV string voltage is not equally distributed among the PV modules, see Fig. 5c and Fig. 5d. Finally, the voltages at *P2* and *P1* are nearby a multiple of the single module V_M.

Table III summarizes a set of shading conditions affecting the PV string with individual irradiances *G1-G3*, the magnitudes of the current *I*(A), voltage *V*(V), and the GMPP (W). Fig. 4 and Fig. 5 display the characteristics for irradiance conditions A and B in Table III, respectively. Fig. 6a and Fig. 6b show the expected behavior for conditions C and D, respectively. Since these shading conditions have three irradiance levels for the modules, the *I-V* curves have three current levels, and the *P-V* curves have three power peaks. The B condition is a critical shading case that pushes the real

[2] 1.0 Sun: 1000 W/m^2

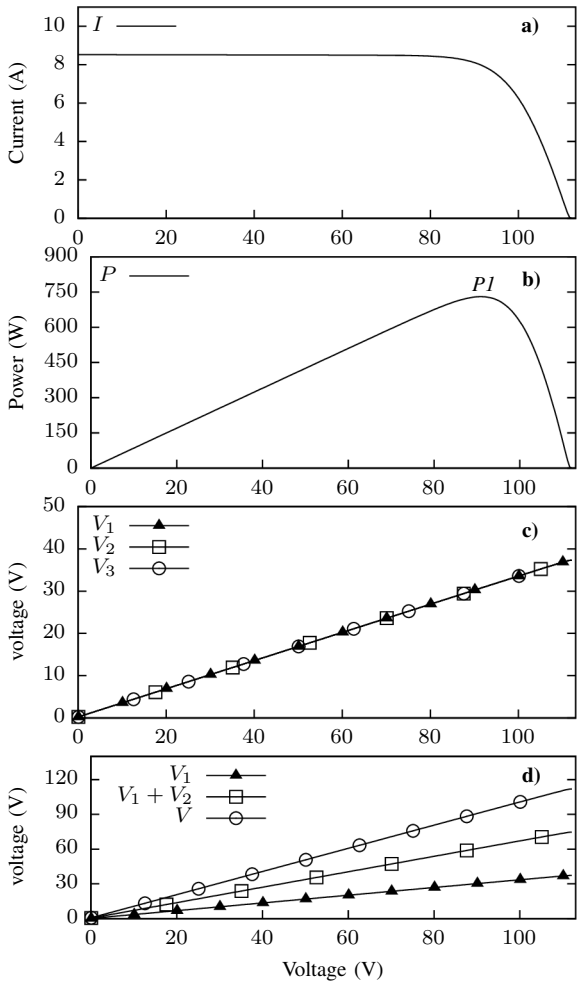

Fig. 4: Characteristic curves of a 730 W PV string with *G1*=*G2*=*G3*=1.0 Sun under UIC.

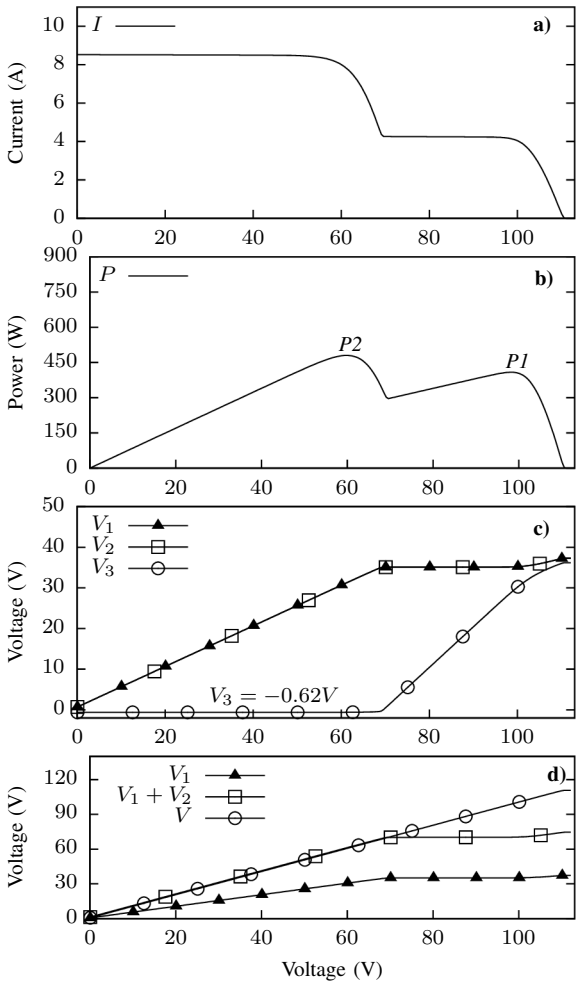

Fig. 5: Characteristic curves of a 730 W PV string with *G1*=*G2*=1.0 Sun and *G3*=0.5 Sun under PSC.

GMPP from the right-side to the left-side of the *P-V* curve with a single jump. The condition C is another critical condition that shapes three power peaks and displaces the GMPP about the center of the *P-V* curve. As shown by the mentioned figures, this shading profile allow the GMPP to lodge at the left side, center region, and the right side of the *P-V* curve, so that a MPPT algorithm has to do a more complex task than under uniform illumination conditions (condition A).

Fig. 7 shows the expected response of the IC algorithm to the shading conditions in Table III varying in time. The traces of the current, voltage and power of the PV string show its average value for each condition. At *t=0* s the PV system is under condition A, the averaged current is 8.02A, the averaged voltage is 90.99V, and the averaged maximum power is 723.30W which is nearby the GMPP. At *t=0.5* s, the condition B shows up, the average current becomes 4.15A, the average voltage is 98.30V, and the averaged maximum power is 404.45W which is far away from the GMPP at *P2*, but close to the local maximum power point *P1*, see Fig. 5b. Then, in this case, the IC algorithm misses the authentic GMPP given in Table III. At *t=1.0* s, the condition C occurs in the PV string, the average current is now 2.11A, the average voltage is 89.22V, and the averaged maximum power is 188.34W which is distant from the GMPP at *P2*, but close to the local maximum power point at *P3*, see Fig. 7c. Finally, at *t=1.5* s the condition D appears upon the PV string, the average current is 6.63A, the average voltage is 93.71V, and the averaged maximum power is 615.53W which is adjacent to the GMPP. As shown, the IC algorithm misses the real GMPP for the shading conditions B and C. Moreover, the traces of current, voltage, and power have a considerable ripple that reduces the MPPT efficiency since d_{step} is a constant term for this algorithm.

TABLE III
SHADING CONDITIONS AND THE RESPECTIVE GMPP

Condition	*G1* (Sun)	*G2* (Sun)	*G3* (Sun)	*I* (A)	*V* (V)	GMPP (W)
A	1	1	1	8.03	90.90	730.49
B	1	1	0.5	8.03	59.80	480.28
C	1	0.25	0.5	4.12	63.30	260.75
D	1	0.9	0.8	6.64	93.70	622.27

Fig. 8 shows the behavior of the AIC algorithm under the

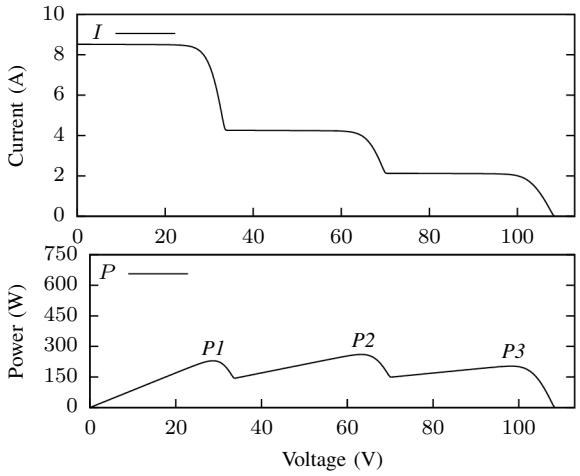

(a) Condition C

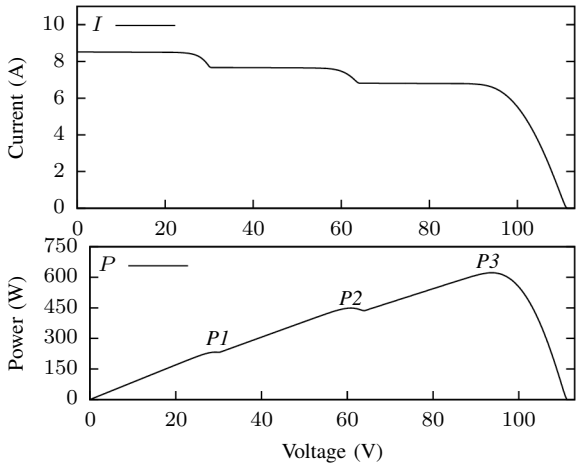

(b) Condition D

Fig. 6: Characteristic curves of 730 W PV string.

shading conditions given in Table III. At *t=0* s, the condition A gets on the PV modules, the average current is 8.03A, the average voltage is 90.90V and the averaged maximum power is 730.47W which is very close to the ideal GMPP. At *t=0.5* s, the shading condition B occurs, and the average current is 8.02A, the average voltage is 59.83V and the averaged maximum power is 480.27W which is almost *P2* of Fig. 5b. At *t=1.0* s, the condition C occurs in the PV string, and the average current is 4.12A, the average voltage is 63.25V and the average maximum power is 260.48W which again is very close to the ideal GMPP. At *t=1.5* s the shading condition D shows up; the average current is 6.64A, the average voltage is 93.68V and the average maximum power is 622.25W which agrees with the GMPP. Therefore, the AIC algorithm successfully tracks the PV string GMPP under this shading profile.

Table IV shows the optimized parameters and the resulting dynamic MPPT efficiencies for the IC and AIC algorithms. It is clear the conventional IC algorithm originally proposed for uniform irradiance conditions (UIC), provide a low MPPT efficiency of only 83.28%, because it is not able to follow

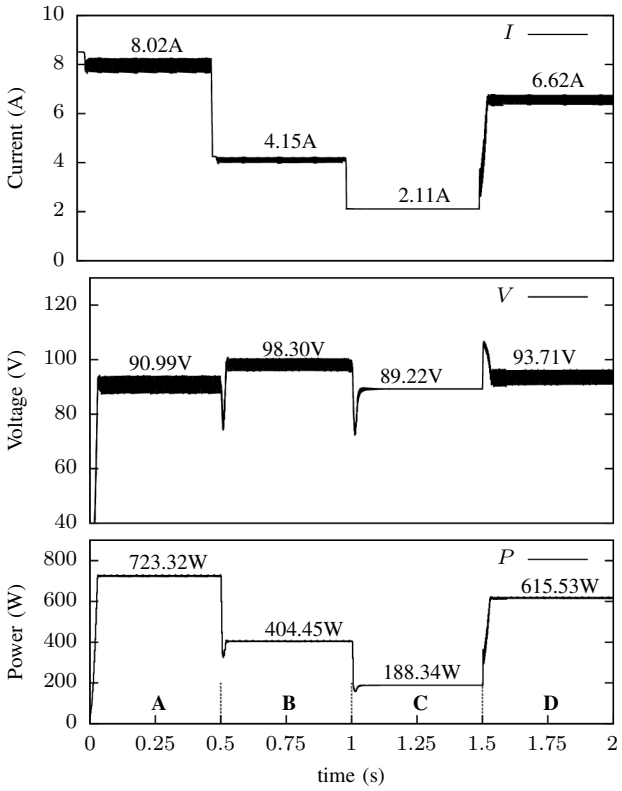

Fig. 7: Response for the IC algorithm of a 730 W PV system under the shading conditions in Table III.

the GMPP under the critical shading conditions B and C. In contrast, the AIC algorithm successfully follows the GMPP for all the shading conditions in Table III, but it differs by a small 0.3% from the simulated 99.6% MPPT efficiency reported in [9] for a pure uniform irradiance condition.

TABLE IV
PARAMETERS AND MPPT EFFICIENCIES FOR THE IC AND AIC ALGORITHMS

Algorithm	$\mathbf{d_{step}}$	$\mathbf{T_S}$ **(s)**	$\mathbf{N_{AIC}}$	$\eta_{\mathbf{mppt}}$ **(%)**
IC	0.012	0.002	-	83.28
AIC	-	0.001	0.035	99.34

V. CONCLUSION

In this work, modeling and simulation of a PV string under shading conditions was carried out. Each PV module under shading requires a bypass diode to keep a reliable path for the current and the PV string operation. The shadowed PV modules cause the following facts on the entire PV string behavior: the *I-V* curve has multiple steps; the number of steps for the *I-V* curve equals the number of irradiance levels on the modules; the number of power peaks for the *P-V* curve equals the number of *I-V* steps, but only one becomes the global maximum power point (GMPP); the voltage at an obscured PV module is identical to the negative bypass diode polarization; the magnitude of the GMPP decreases according to the shading shape, but the voltage at the GMPP appears nearby a multiple of the single PV module voltage Vm. The

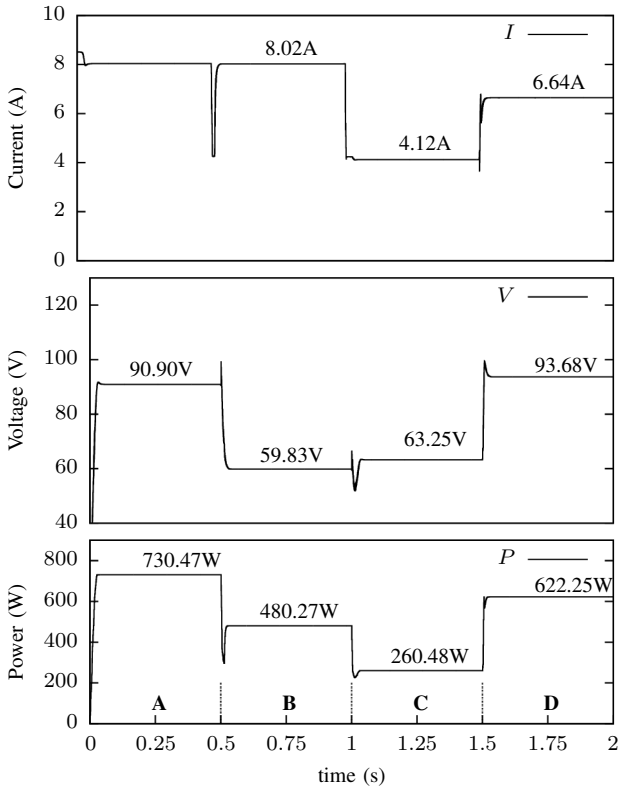

Fig. 8: Response for the AIC algorithm of a 730 W PV system under the shading conditions in Table III.

employed simulation allowed us to observe the behavior of the conventional IC and the improved AIC algorithms with a three-module string under the shading pattern described in Table III, and to compare their efficiency responses. The IC algorithm misses the authentic GMPP under the critical conditions B and C where the GMPP is located at the left-side and at the center of the P-V curve, respectively. The resulting MPPT efficiency of the IC algorithm was only 83.28%. In contrast, although originally proposed for PV modules under uniform irradiance conditions, the AIC algorithm successfully tracks the real GMPP under all conditions of the proposed shading profile. It shows very good power tracking during solar irradiance transients and steady states, and the MPPT efficiency of the AIC algorithm is around 99.34%. This is a very high-power tracking efficiency, comparable to more complex soft computing and bio-inspired methods, but the AIC is simpler to implement than those alternative algorithms. Having experimental confirmation of the results shown here would require a very specialized laboratory; then, in the future, we shall obtain experimental results by using at least 3 PV module emulators (controlled by a computer) working in the same conditions simulated in this work.

REFERENCES

[1] S. Saravanan and N. R. Babu, "Maximum power point tracking algorithms for photovoltaic system - A review," Renewable and Sustainable Energy Rev., vol. 57, pp. 192-204, 2016, DOI: https://doi.org/10.1016/j.rser.2015.12.105.

[2] P. Joshi and S. Arora, "Maximum power point tracking methodologies for solar PV systems – A review," Renewable Sustainable Energy Rev., vol. 70, pp. 1154-1177, 2017, DOI: https://doi.org/10.1016/j.rser.2016.12.019.

[3] J. P. Ram, T. S. Babu and N. Rajasekar, "A comprehensive review on solar PV maximum power point tracking techniques," Renewable Sustainable Energy Rev., vol. 67, pp. 826-847, 2017, DOI: https://doi.org/10.1016/j.rser.2016.09.076.

[4] F. Belhachat and C. Larbes, "A review of global maximum power point tracking techniques of photovoltaic system under partial shading conditions," Renewable Sustainable Energy Rev., vol. 92, pp. 513-553, 2018, DOI: https://doi.org/10.1016/j.rser.2018.04.094.

[5] M. A. Danandeh and G. S.M. Mousavi, "Comparative and comprehensive review of maximum power point tracking methods for PV cells," Renewable Sustainable Energy Rev., vol. 82, pp. 2743-2767, 2018, DOI: 10.1016/j.rser.2017.10.009.

[6] L. L. Jiang, R. Srivatsan and D. L. Maskell, "Computational intelligence techniques for maximum power point tracking in PV systems: A review," Renewable Sustainable Energy Rev., vol. 85, pp. 14-45, 2018, DOI: 10.1016/j.rser.2018.01.006.

[7] Guiqiang Li, Yi Jin, M.W. Akram, Xiao Chen, Jie Ji, "Application of bio-inspired algorithms in maximum power point tracking for PV systems under partial shading conditions – A review," Renewable and Sustainable Energy Reviews, vol. 81, pp. 840-873, 2018, ISSN 1364-0321, DOI: 10.1016/j.rser.2017.08.034.

[8] R. B. Bollipo, S. Mikkili and P. K. Bonthagorla, "Hybrid, optimal, intelligent and classical PV MPPT techniques: A review," CSEE J. Power Energy Syst., vol. 7, pp. 9-33, 2021, DOI: 10.17775/CSEEJPES.2019.02720.

[9] A. Morales-Acevedo, J. L. Diaz-Bernabe and R. Garrido-Moctezuma, "Improved MPPT adaptive incremental conductance algorithm," in Proceedings IEEE IECON 2014, Dallas, TX, USA, 2014, pp. 5540-5545, DOI: 10.1109/IECON.2014.7049347.

[10] D. Sera, R. Teodorescu and P. Rodriguez, "PV panel model based on datasheet values," in IEEE ISIE 2007, pp. 2392–2396, 2007. DOI: 10.1109/ISIE.2007.4374981.

[11] H.-L. Tsai, C.-S. Tu and Y.-J. Su, "Development of generalized photovoltaic model using MATLAB/SIMULINK," in Proceedings WCECS 2008, San Francisco, USA, 2008. pp. 1–6.

[12] L. Castañer and Santiago Silvestre, "Solar Cell Arrays, PV modules and PV generators," in Modelling Photovoltaic Systems Using PSpice, John Wiley &Sons Ltd, 2002, Ch. 4, pp. 91-96, DOI:10.1002/0470855541.

[13] D. Maksimovic, A. M. Stankovic, V. J. Thottuvelil and G. C. Verghese, "Modeling and simulation of power electronic converters," in Proceedings of the IEEE, vol. 89, no. 6, pp. 898-912, 2002, DOI: 10.1002/0470855541.ch4

[14] J. L. Díaz-Barnabé and A. Morales-Acevedo, "Experimental study of the equivalence of the Adaptive Incremental Conductance (AIC) and the Adaptive Perturb and Observe (APO) algorithms for PV systems maximum power tracking," IEEE Lat. Am. Trans., vol. 17, pp. 1237-1243, 2019, DOI: 10.1109/TLA.2019.8932331.

[15] D. P. Hohm and M. E. Ropp, "Comparative study of maximum power point tracking algorithms," Prog. Photovolt. Res. Appl., vol. 11, pp. 47–62, 2003, DOI: 10.1002/pip.459.

[16] T. S. Hub, Suntech STP245S-20/WD PV module Datasheet, [Online]. Available: http://www.solarhub.com/solarhub_products/29548-STP245S-20-Wdb-Suntech-Power, Accessed on: Apr. 5, 2021.

[17] M. H. Rashid, "Behavioral Device Modeling," in SPICE for power electronics and Electric Power, Third ed. Boca Raton, FL., USA, CRC Press, 2012, Ch. 4, Sec. 4.5, pp. 85–97.

[18] Holger Vogt, Marcel Hendrix, and Paolo Nenzi, "Mixed-Mode and Behavioral modeling with XSPICE," in Ngspice User's Manual Version 37, 2022, Ch. 12, pp. 177-276, [Online]. Available: https://ngspice.sourceforge.io/docs/ngspice-37-manual.pdf.